Research on Engineering Structures & Materials
www.jresm.org
Research Group

Research Article

Bond behavior enhancement between normal strength concrete and SIFCON

Ali Fahdel [*,a] Kamal Alogla [b], Wajdi Shubber Saheb [c]

College of Engineering, University of Kerbala, Kerbala, Iraq

Article Info

Article History:

Received 02 Feb 2026

Accepted 15 Apr 2026

Keywords:

Push-off test;
Steel fibers;
Interface behavior;
Slurry infiltrated fiber concrete;
Fiber reinforced concrete;
Shear strength

Abstract

The bonding behavior between conventional concrete and Slurry Infiltrated Fiber Concrete (SIFCON) plays a critical role in enhancing the shear performance and ductility of composite structural members. This study investigates seven reinforced concrete specimens, divided into two groups in addition to a control sample made entirely of conventional concrete. The first group consisted of three composite beams combining conventional concrete and SIFCON, cast separately and connected through different interfacial geometries: rectangular, triangular, and semicircular. The second group replicated these specimens with the addition of 12 mm diameter bolts at the interface to improve bond strength. The results demonstrated that interface geometry significantly influences shear resistance and displacement behavior. Among the tested configurations, the rectangular interface achieved the highest performance, with a shear capacity increase of approximately 2.38 times compared to other shapes, along with improved stiffness and ductility. The inclusion of bolt reinforcement further enhanced load-carrying capacity, reaching about 1.6 times that of specimens without bolts. These specimens also exhibited larger displacements and interfacial slip prior to failure. However, despite the increased strength, bolt-reinforced specimens showed a more brittle and sudden failure mode, unlike the more gradual and ductile response observed in specimens with rectangular interfaces without bolts. The findings confirm that combining mechanical interlocking with anchorage systems can effectively improve shear strength and deformation capacity. Future research should focus on large-scale applications and long-term performance under cyclic and sustained loading conditions.

1. Introduction

Modern civil engineering relies heavily on concrete as the primary construction material due to its durability, high compressive strength, cost-effectiveness, and widespread availability [1–3]. Despite these advantages, combining different types of concrete within a single structural element—such as in repair works, strengthening applications, or staged construction—often leads to weak interfacial performance. In particular, conventional concrete design provisions indicate that the interface between old and new concrete may exhibit limited shear stress resistance and inadequate bond capacity [4,5]. These deficiencies can adversely affect the overall strength, stiffness, and long-term serviceability of reinforced concrete members [6,7].

The performance of composite concrete systems is largely governed by the behavior of the interface zone, where shear transfer mechanisms play a decisive role. Load transfer across construction joints typically depends on a combination of adhesion, friction, and mechanical interlocking. Surface roughness enhances aggregate interlock, while normal compressive stresses mobilize frictional resistance. In many cases, additional reinforcement crossing the interface is

*Corresponding author: kamal.d@uokerbala.edu.iq
[a]orcid.org/0009-0001-5065-2301; [b]orcid.org/0000-0002-0853-5152; [c]orcid.org/0000-0002-7069-3207
DOI: http://dx.doi.org/10.17515/resm2026-1492me0202rs

required to provide dowel action and prevent slip. However, the efficiency of these mechanisms is influenced by surface preparation, material compatibility, and the presence of mechanical connectors, making the interface a critical and often vulnerable region in composite members.

To overcome such limitations, various high-performance concrete materials have been developed [8–10]. Among them, Slurry Infiltrated Fiber Concrete (SIFCON) has emerged as a promising material due to its unique production method and superior mechanical characteristics [11,12]. SIFCON is produced by first placing a high-volume fraction of short steel fibers—typically ranging from 4% to 20%—into a mold, followed by infiltrating a highly flowable cementitious slurry composed of fine cement, silica fume, water, and superplasticizer [13–15]. Unlike conventional Fiber Reinforced Concrete (FRC), where fibers are mixed directly into fresh concrete, SIFCON achieves a significantly higher and more uniformly distributed fiber content through this preplacement technique [16,17]. This distinctive fiber network results in exceptional ductility, impact resistance, energy absorption capacity, shear strength, crack control, and fatigue performance [18–21]. The interconnected fibers bridge microcracks effectively, improving post-cracking behavior and stress redistribution under severe loading conditions. Consequently, SIFCON has been successfully applied in blast-resistant structures, repair systems, joint regions, and shear-critical zones [22–24].

Although extensive research has examined the intrinsic mechanical properties of SIFCON, relatively limited attention has been devoted to its bond behavior when combined with conventional concrete, particularly in terms of shear transfer and interface strength [25–27]. Previous studies on construction joints have explored methods such as surface roughening, keyways, shear reinforcement, and mechanical connectors to enhance interfacial performance [28–30]. Nevertheless, the interaction between SIFCON and normal concrete at the interface—especially under varying geometric configurations and mechanical anchorage systems—remains insufficiently understood. Therefore, achieving optimal interfacial bonding in hybrid systems incorporating SIFCON layers requires systematic investigation. The geometry of the interface surface may significantly influence mechanical interlocking, while bolted or dowel-type connectors can provide additional shear resistance through mechanical anchorage. Understanding the combined effect of geometric interlock and mechanical fastening is essential for developing reliable and efficient composite systems.

The primary objective of this study is to evaluate the effect of using Slurry Infiltrated Fiber Concrete (SIFCON) on shear-friction resistance at construction joints between old and new concrete. This includes examining the influence of different interface surface configurations (rectangular, semicircular, and triangular) and employing various shear transfer mechanisms across the interface, such as dowel bars and bolted connections, in addition to investigating a hybrid system that combines geometric interlocking with mechanical anchorage.

2. Experimental Program

Seven reinforced concrete beam specimens were produced for experimental testing and divided into three separate groups. This study is exploratory in nature, aiming to investigate and better understand the interfacial shear behavior between conventional concrete and SIFCON through controlled laboratory experimentation. The first group contained one specimen which acted as the control model to represent standard concrete construction. The specimen served as a reference point to assess the enhanced shear performance of the following specimens. The control specimen consisted of two separate conventional concrete sections which were cast separately to create a single beam structure.

The second group consisted of three composite specimens which combined conventional concrete with Slurry Infiltrated Fiber Concrete (SIFCON) in two separate sections. The two separate sections of material received individual casting before their interface received special treatment to improve mechanical bonding. The three specimens used different interface shapes for their interlocking design: rectangular for the first specimen, triangular for the second, and semicircular for the third, as shown in Figures (1) and listed in Table (1). The researchers studied how different interface shapes between conventional concrete and SIFCON affect their shear transfer and bond

performance. The third group consisted of three specimens derived from the second group before receiving additional reinforcement through 12 mm diameter steel bolts that spanned the interface area. The steel bolts served to establish mechanical bonds between the interface zones for all three interlocking designs, which strengthened interface shear capacity and minimized interface slip. The complete details about these specimens appear in Figures (1) and Table (1). The experimental design allowed researchers to study how different interface shapes and mechanical fasteners affect beam composite performance when conventional concrete meets SIFCON under shear stress. All tests were carried out in the Laboratory of Karbala University.

Table 1. Details of the tested specimens

Groups	Parameter	Specimen Designation	Mixture Type
first group	Reference	N. L	N.C - N.C
second group (Change Interface)	Rectangle Grooves	S. R	N.C - SIFCON
	Triangle Grooves	S. T	N.C - SIFCON
	Semicircular Grooves	S.C	N.C - SIFCON
third group (Change Interface with Bolts)	Rectangle Grooves with Two bolts of a diameter of 12 mm	S. R. D	N.C - SIFCON
	Triangle Grooves with Two bolts of a diameter of 12 mm	S. T. D	N.C - SIFCON
	Semicircular Grooves with Two bolts of a diameter of 12 mm	S. C. D	N.C - SIFCON

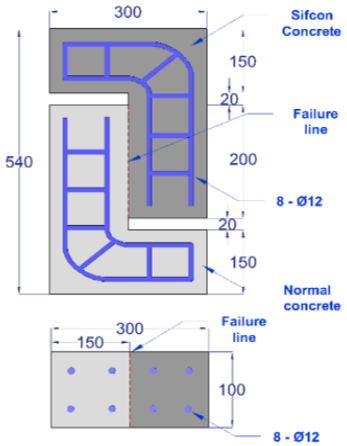

(a)

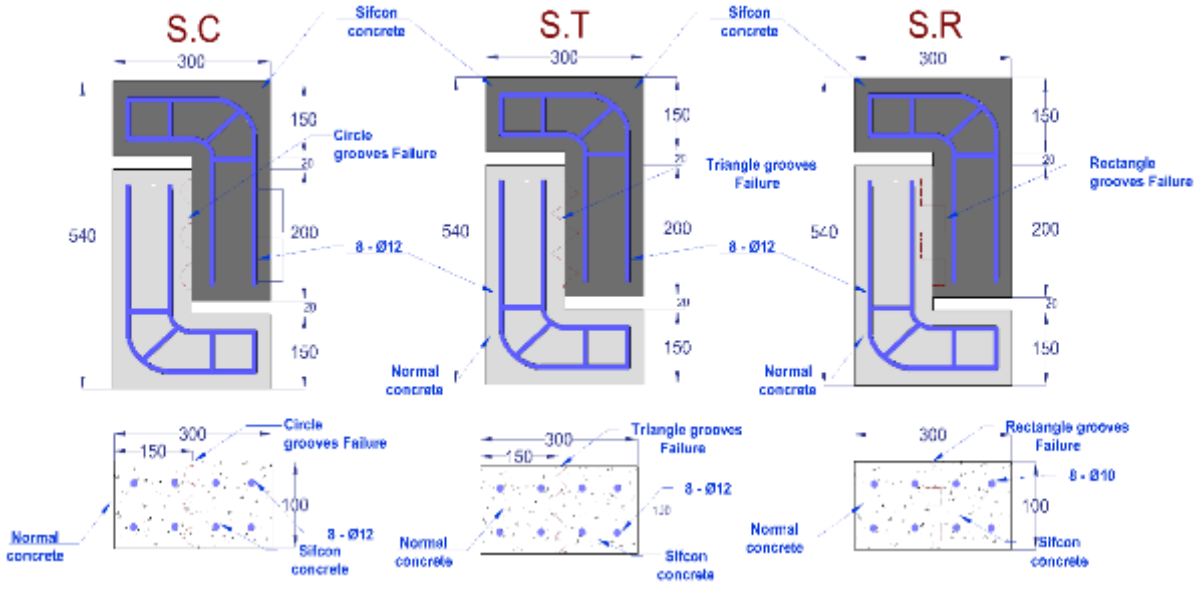

(b) (c) (d)

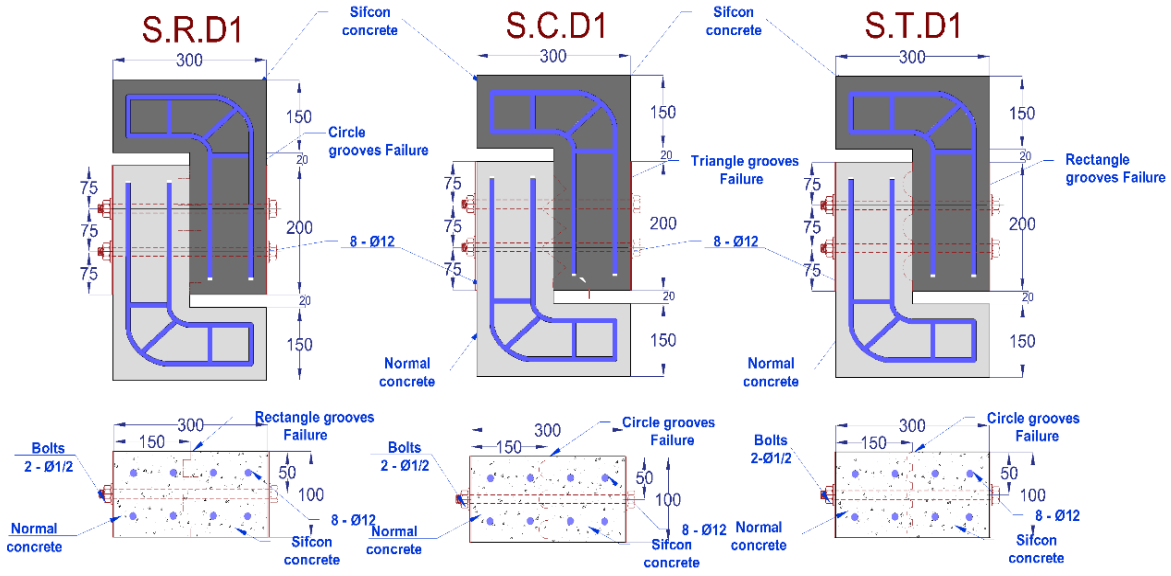

(e) (f) (g)

Fig. 1. Details of the tested specimens (a) Reference, (b) Circle grooves, (c) Triangle grooves, (d) Rectangle grooves, (e) Triangle grooves With Two bolts with a diameter of 12 mm, (f) Triangle grooves With Two bolts with a diameter of 12 mm, and (g) Circle grooves With Two bolts with a diameter of 12 mm

2.1 Preparation of Beam Specimens

The wooden molds for the mix were prepared, and the casting surfaces were oiled. The reinforcement for the specimen was arranged as shown in Figure (2). Subsequently, the conventional concrete mix was prepared, and the first portion of the conventional concrete was cast, as illustrated in Figure (3). After that, the SIFCON mix was prepared and cast, as shown in Figure (4). To ensure reproducibility and consistency in the experimental results, the curing procedure of the concrete specimens was carefully controlled. After casting, all specimens were subjected to water immersion curing to guarantee full hydration and uniform moisture distribution. The specimens were completely submerged in clean water tanks for a duration of 28 days. The water temperature was maintained at 20 ± 2°C throughout the curing period to provide stable and controlled conditions, in accordance with standard concrete testing practices (e.g., ASTM C192 or EN 12390-2).

Fig. 2. Preparation of plywood formwork and reinforcement

Fig. 3. Casting the first segment of conventional concrete

Fig. 4. Casting the second segment of SIFCON concrete

3. MATERIAL

3.1. Cement

The research used Al-Jisir cement which is a well-established Iraqi product that meets all requirements of the Iraqi Standard [IQS No. 5/2019]. The research used Type V sulfate-resistant Portland cement which meets the following specifications: 600 minutes maximum setting time and 32 MPa minimum compressive strength at 28 days and 4% maximum sulfate content by weight according to the standard specifications. The cement properties listed in Tables (2) and (3) match all Type V cement requirements from IQS No. 5/2019 thus making it appropriate for sulfate-rich environments.

Table 2. Sulfate-resistant Portland cement's chemical and key ingredients

Oxide's composition	Content%	Limits of Iraqi standard No.5/2019
CaO	62.14	.....
SIO2	19.90	.....
AL2O3	3.3	.....
Fe2O3	4.5	.....
MgO	3.25	<5.00
SO3	1.86	<2.50
Na2O	0.24	
K2O	0.53	
L.O.I.	1.27	<4.00
Insoluble residue	0.81	<1.5
Lime Saturation factor	0.93	0.66-1.02
Main compounds (Bongu 'equations)		
C3S	62.12	.....
C2S	19.84	.....
C3A	3.52	<3.50
C4AF	4.76	.....

Table 3. The properties Physical characteristics of cement

Physical properties		Test Results	Limits of Iraqi Standard No.5/2019
Surface area (Blaine)m^2/kg		281	≥250
Setting time (min.)	Initial setting	232	≥45
	Final setting	297	≤600
Compressive strength, MPA	2-day	24.7	≥10
	28-day	39.67	≥32.5R
Soundness (Autoclave)%		0.14	≤0.8

3.2 Fine Aggregate

The research used Zone 2 Natural fine aggregate which met the requirements of the Iraqi Standard [IQS No. 45/1984] and came from the Maqale Karbala factory. The fine aggregate particle size distribution appears in Tables (4) which show that the material meets all grading specifications from IQS No. 45/1984. The fine aggregate meets concrete production requirements according to the physical and chemical properties presented in Table (5).

Table 4. The properties physical and chemical of the fine aggregate utilized

Sieves size (mm)	The passing Percentage of fine aggregate	Limits of (IQS. No.45/1984) (Zone 2)	
		Min. Limit	Max. Limit
10	100	100	100
4.75	96	90	100
2.36	90	85	100
1.18	82	75	90
0.6	75	60	79
0.3	42	40	12
0.15	1.2	0	10

Table (5). Grading of the of fine aggregate used

Characteristics	Test results	Limits of (IQS. No. 45/1984
Sulfate content (SO3) %	0.323	0.5% (max.)
Material finer than 75 µm	1.82	5% (max.)
Specific gravity	2.69	---
Absorption %	0.81	---
Fineness modulus	---	---

3.3 Coarse Aggregate

In this study, pre-graded gravel with a nominal maximum size of 20 mm, obtained from the Al-Niba'ai region, was utilized as the coarse aggregate. Prior to incorporation into the mixes, the aggregate was thoroughly washed to eliminate surface dust and subsequently air-dried until reaching a saturated surface-dry (SSD) condition. The results of the sieve analysis and the corresponding grading curve for the coarse aggregate, conducted in compliance with the Iraqi Standard (IQS No. 45/1984), are presented in. Furthermore, the chemical and physical properties of the gravel, as detailed in Table (6) and (7), respectively, were found to be fully consistent with the specified requirements of the same standard

Table 6. Grading of the coarse aggregate used

Sieves size (mm)	The passing Percentage of fine aggregate	Limits of (IQS. No.45/1984) grade 5-14 mm	
		Min. Limit	Max. Limit
37.5	100	100	100
20	96	95	100
9.5	37	30	60
5	2	0	10

Table 7. The physical and chemical of the coarse aggregate used

Characteristics	Test results	Limits of (IQS. No. 45/1984)
Sulfate content (SO3) %	0.045	0.1% (max.)
Material finer than 75 µm	0.063	3% (max.)
Specific gravity	2.62	---
Absorption %	0.79	---

3.4 Water

Clean, potable tap water was utilized throughout the experimental procedures, including the washing of and coarse aggregate samples, as well as for the mixing, casting, and curing of concrete specimens.

3.5 Silica Fume

Nano Silica (Grade A) – MAXPOWDER is spherical with a particle size of 229 nm and a high specific surface area of 20–25 m^2/g. It exhibits a real density of 1.9 g/cm^3 and a bulk density ranging from 300–500 kg/m^3. The material has a high melting point of 1230 °C. Its chemical composition is predominantly SiO_2 (90–95%), with minor amounts of Al_2O_3, Fe_2O_3, C, Na_2O, K_2O, MgO, S, CaO, MnO, P_2O_5, and traces of LOI and moisture, maintaining a pH between 6.8 and 8.

3.6 Steel Reinforcement

In this research, two different sizes of Deformed bars were used. One was a 12 mm diameter bar for longitudinal reinforcement, while the other was an 8 mm diameter bar for transverse reinforcement (stirrups). The test results of steel bars are shown in the Tables (8), which are in accordance with the requirements of ASTM A615/A615M.

Table 8. Steel reinforcement properties

Properties	Results		Tensile requirement ASTM 615M – 05a (Minimum)	
Nominal diameter (mm)	Ø12	Ø 8	Grade 60	Grade 40
Actual diameter (mm)	12	8	-	-
Yield stress, fy (MPa)	479.6	411.8	420	280
Ultimate stress, fu (MPa)	634.6	640.9	620	420
Elongation %	17.6	23.9	7-9	11-12

3.7 Steel Fiber

The steel fibers employed in this study were straight-ended and of micro size, with a length of 6 mm and a diameter of 0.2 mm, resulting in an aspect ratio of .30 These fibers exhibited a tensile strength of 2,850 MPa, a density of 7.85 g/cm^3, Table (9): Steel Fiber properties

Table 9. Steel Fiber properties

Description	Micro copper coated steel fiber (Model HX-DT-S01)
Length	6 – 20 mm
Diameter	0.2 – 0.3 mm (Optional: 0.18 – 0.5 mm)
Type	Straight wire / Hooked end
Color	Copper coated
Material	Steel wire
Tensile Strength	≥ 2850 MPa

3.8 Superplasticizer (SP)

The research utilized Structure 502 which is a polycarboxylate ether (PCE)-based superplasticizer obtained from Fosroc. The high-performance admixture improves cement particle distribution through electrostatic repulsion and steric hindrance which results in lower water requirements and better flowability. The product delivers superior water-reducing capabilities and maintains excellent workability properties which suit applications involving high-performance and highly flowable concrete mixes. The essential technical characteristics of the product appear in Table (10).

Table 10. Structure 502 (Fosroc) technical data*

Properties	Value or Description
Appearance	Light brown colored liquid
PH value	6.5
S.G. @ 20-C	1.06 ± 0.02
Chloride content	Nil
Alkali content	Typically, less than 1.5 gm Na_2O equivalent per liter of admixture

**The manufacturer provides this info. Fosroc*

3.9 Mix Proportions

The research examines how conventional concrete interacts with SIFCON when used together. The research focused on creating better bond strength between these two materials through the variables listed. The research used the conventional concrete mix design from Table (11) and developed the SIFCON mix design which appears in Table (11). The research study [31] provided the necessary mix properties for this investigation.

Table 11. Mix proportions

Mix No.	Type of Mix	Cement (kg/m^3)	Coarse aggregate (kg/m^3)	Fine aggregate (kg/m^3)	Silica Fume (kg)	Water (L/m^3)	Steel Fiber (kg/m^3)	Super-plasticizer liters per 100 kg
1	Normal Concrete	400	1050	850	------	180	-----	0.2 to 3.0 of cementitious materials.
2	SIFCON	1000	------	1000	0.1 from cement	300	6% From the size of the concrete	0.2 to 3.0 of cementitious materials.

4. Testing Procedure

The testing apparatus required three reinforced concrete beams for precise experimental testing through repeated experimental procedures. The testing procedure followed a structured approach to achieve both precise results and dependable outcomes. The entire testing equipment received thorough installation of all its components including sensors and mechanical parts into their assigned locations. 1. The steel support frame received pin and roller supports at its base to achieve stable and precise beam fixation. 2. The load cell received its placement at beam center point while the LVDT displacement sensor operated from a position directly under the beam's midspan to measure load and Interfacial Slip accurately. 3. The load distributor rested on top of the beam to distribute the applied force evenly throughout its width. 4. The testing system became operational after integration with the electronic control system which enabled digital load control through the control program. 5. The load cell tracked the applied force throughout the loading process while the LVDT sensor measured Interfacial Slip with high precision. The experimental data about beam structural behavior under loading conditions became available through this testing arrangement.

4.1 Hardened Tests

4.1.1. Compressive Strength Test

The compressive strength test was conducted on cubic specimens measuring 150 × 150 × 150 mm for each concrete mixture at curing ages of 7 and 28 days, in accordance with BS 1881: Part 116 (1981). The test was performed using a compression testing machine with a capacity of 2000 kN. For each mixture, the compressive strength was determined as the average value of three specimens, calculated using the standard formula.

The results indicated that the compressive strength of SIFCON concrete was significantly higher than that of conventional concrete. This improvement is primarily attributed to the high-volume fraction of steel fibers incorporated into the SIFCON matrix, as presented in Table (12). The notable increase in strength can be explained by the efficient infiltration of the cementitious slurry into the densely packed steel fibers, leading to the formation of a homogeneous and well-bonded composite material.

Table 12. Results of the tested mixtures' cube's compressive strength after 7 and 28 days

No. Mix	Mixture symbols	Cube Compressive strength (*f*cu), MPa	
		At 7 Days	At 28 Days
1	N	38	49
2	S	51	77

4.1.2. Splitting Tensile Strength

The ASTM C496 standard guided the splitting tensile strength evaluation of 200 × 100 mm cylindrical specimens at 7 and 28 days of curing. The testing procedure involved placing each cylinder between two wooden bearing strips which maintained equal force distribution across the upper and lower surfaces. The splitting tensile strength calculation used the standard method from ASTM C496 to determine the average value from three specimens. The test results in Table (13) show that SIFCON specimens demonstrated higher tensile strength than standard concrete specimens. The high steel fiber content in the specimens led to better tensile stress resistance and enhanced their ability to bridge cracks throughout the matrix.

Table 13. Results of splitting Tensile strength at 7 and 28 days

No. Mix	Mixture symbols	Splitting tensile stress (*f sp*), MPa	
		At 7 Days	At 28 Days
1	N	12	13
2	S	14	20

4.1.3. Modulus of Rupture

The flexural strength test used 100 × 100 × 400 mm prismatic specimens to evaluate their performance at 7 and 28 days of curing age according to ASTM C78-02. The flexural testing machine with 150 kN capacity executed the test by applying two-point loading to the specimens. The ASTM C78 formula enabled the calculation of modulus of rupture to determine the average value from two specimens. The experimental results in Table (14) demonstrate that SIFCON mixture outperformed conventional concrete by achieving a 500% strength improvement. The SIFCON specimens withstood flexural loading tests better than conventional concrete specimens because they displayed minimal cracking during the tests.

Table 14. Results of Modulus of rupture at 7 and 28 days

NO. mix	Mixture symbols	Modulus of rupture (*fr*), MPa	
		At 7 Days	At 28 Days
1	N	12.8	13.28
2	S	15.4	21.16

4.2. Beam Specimen Design for Experimental Results

The improvement of shear strength in separate beam sections represents a critical need for structural maintenance work and strengthening operations of damaged structural elements under unexpected loading conditions. The research used high-performance materials to boost shear resistance through multiple strengthening methods which improved bond strength and stress distribution between structural components. The experimental study investigated seven composite specimens which consisted of two parts: conventional reinforced concrete in the first

section and Slurry Infiltrated Fiber Concrete (SIFCON) in the second section. The push-off loading test was applied to all specimens to measure their interfacial shear behavior and the obtained results appear in Table (1). The research measured shear capacity improvement through tests that compared composite specimens to a reference sample made from conventional concrete for both segments. The research showed that the composite specimens demonstrated better shear resistance than the reference sample according to the results presented in Table (15). The researchers organized the specimens into three experimental groups to evaluate their interfacial configurations and strengthening methods.

Table 15. Results of all beams tested

No.	Groups	Specimens	First crack (kN)	Interfacial Slip (mm)	Ultimate Load (kN)	improvement ratio percentage
1.	first group	N. L	18	2.21	40	0
2.	second group	S. R	70	3.5	131	228%
3.	(Change	S. T	55	0.0375	105.86	165%
4.	Interface)	S.C	40	0.0375	65.97	65%
5.	third group	S. R. D	120	2.615	211.28	428%
6.	(Change	S. T. D	95	1.3	161.5	304%
7.	Interface with Bolts)	S. C. D	80	0.6	105.74	164%

4.2.1 First group: Control Specimen (N.L)

The specimen N.L was cast monolithically and considered the reference specimen for comparison with all strengthened specimens as illustrated in Figure (5). The first shear crack appeared at approximately 8 kN, representing about 44% of the ultimate load, and propagated along the shear plane due to the concentration of shear stresses. The specimen ultimately failed at a load of 18 kN.

The load–displacement curve indicated relatively low stiffness and limited shear resistance compared with the strengthened specimens. However, the specimen exhibited a relatively large deformation prior to failure. in Figure 6.

- Peak load ≈ 18 kN
- Ultimate displacement ≈ 2.7 mm
- Energy absorption ≈ 32 J
- Ductility index ≈ 9.0

These results indicate that although the specimen exhibited moderate ductility, its load-carrying capacity and energy dissipation capability were relatively limited.

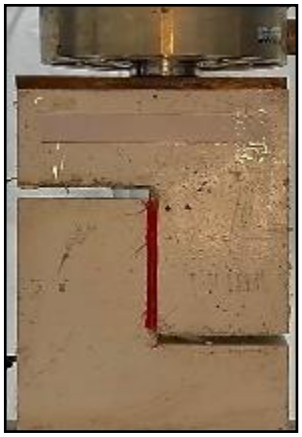

Fig. 5. Control specimen (N.L)

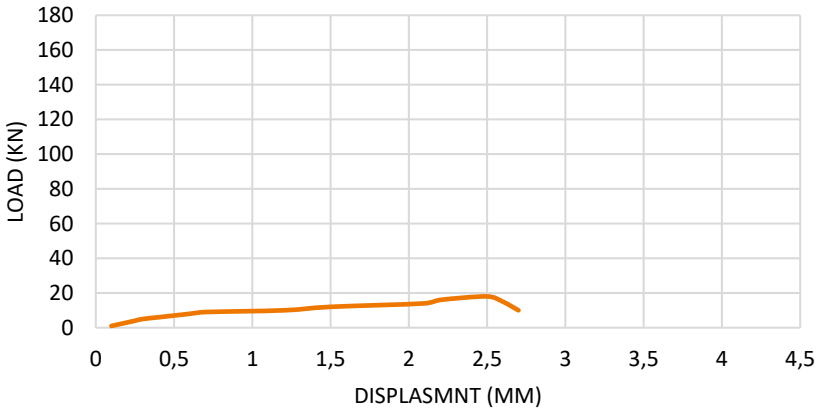

Fig. 6. Control specimen (N.L) Load-Displacement

4.2.2. Second Group: Specimens Reinforced of Change Interface (S. R), (S.T) and (S.C)

Specimen S.T: The triangular groove configuration showed improved shear resistance, as illustrated in Figure (7). The first crack appeared at 45 kN, while the ultimate load reached 105.86 kN. in Figure (8). This configuration demonstrated a good balance between shear capacity and deformation.

- Peak load ≈ 105 kN
- Ultimate displacement ≈ 1.8 mm
- Energy absorption ≈ 145 J
- Ductility index ≈ 9.0

Specimen S.C: The specimen S.C included circular interface grooves as illustrated in Figure (9). The first crack appeared at 35 kN, and the ultimate load reached 65.97 kN in Figure (10). The circular grooves enhanced the mechanical interlock and provided moderate improvement in both strength and ductility.

- Peak load ≈ 65 kN
- Ultimate displacement ≈ 2.4 mm
- Energy absorption ≈ 118 J
- Ductility index ≈ 12.0

Specimen S.R: The rectangular groove specimen exhibited significant improvement in shear strength as illustrated in Figure (11). The first crack appeared at 60 kN, and ultimate failure occurred at 131 kN in Figure (12). The rectangular interface provided strong mechanical interlocking, which enhanced shear transfer capacity.

- Peak load ≈ 130 kN
- Ultimate displacement ≈ 2.2 mm
- Energy absorption ≈ 261 J
- Ductility index ≈ 11.0

Fig. 7. Specimen (S.R)

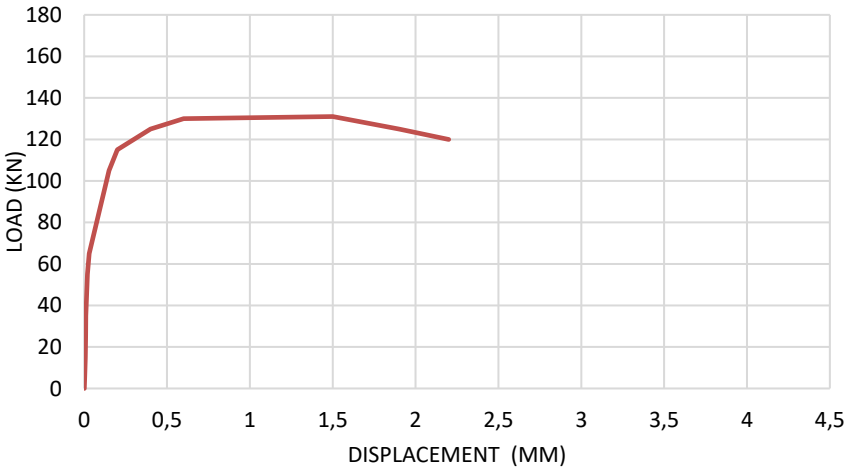

Fig. 8. Specimen (S.R) Load-Displacement

Fig. 9. Specimen (S. T)

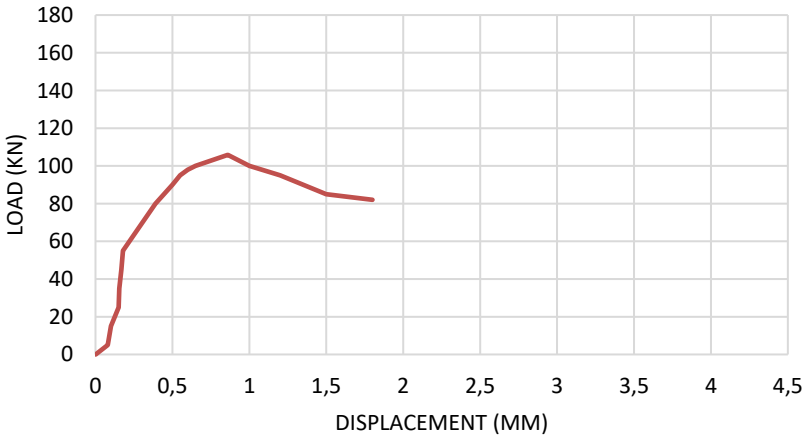

Fig. 10. Specimen (S. T) Load-Displacement

Fig. 11. Specimen (S. C)

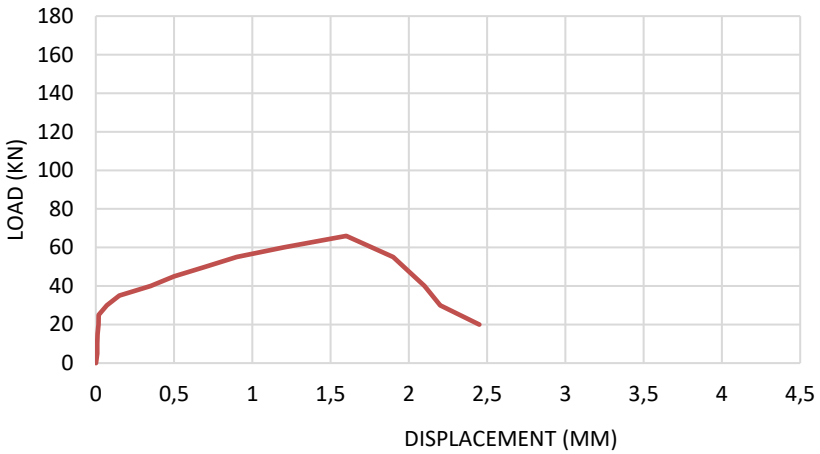

Fig.12. Specimen (S. C) Load-Displacement

4.2.3. Third Group: Specimens Reinforced of Change Interface with Bolts (S.R.D), (S. T.D) and (S.C.D)

Specimen S.T: The triangular groove configuration showed improved shear resistance, as illustrated in Figure (13). The first crack appeared at 45 kN, while the ultimate load reached 105.86 kN. in Figure (14). This configuration demonstrated a good balance between shear capacity and deformation.

- Peak load ≈ 105 kN
- Ultimate displacement ≈ 1.8 mm
- Energy absorption ≈ 145 J
- Ductility index ≈ 9.0

Specimen S.C: The specimen S.C included circular interface grooves as illustrated in Figure (15). The first crack appeared at 35 kN, and the ultimate load reached 65.97 kN in Figure (16). The circular grooves enhanced the mechanical interlock and provided moderate improvement in both strength and ductility.

- Peak load ≈ 65 kN
- Ultimate displacement ≈ 2.4 mm
- Energy absorption ≈ 118 J
- Ductility index ≈ 12.0

Specimen S.R: The rectangular groove specimen exhibited significant improvement in shear strength as illustrated in Figure (17). The first crack appeared at 60 kN, and ultimate failure occurred at 131 kN in Figure (18). The rectangular interface provided strong mechanical interlocking, which enhanced shear transfer capacity.

- Peak load ≈ 130 kN
- Ultimate displacement ≈ 2.2 mm
- Energy absorption ≈ 261 J
- Ductility index ≈ 11.0

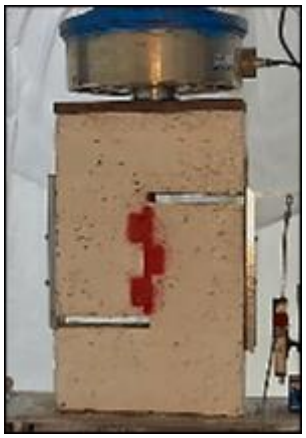

Fig. 13. Specimen (S. R.D)

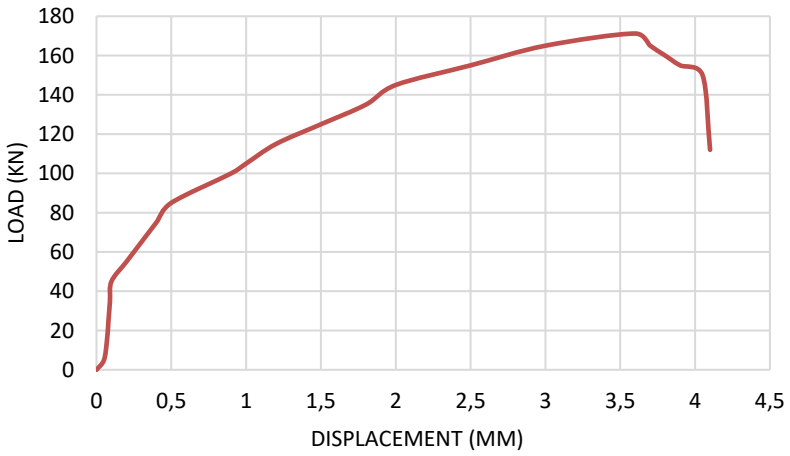

Fig. 14. Specimen (S. R.D) Load-Displacement

Fig. 15. Specimen (S. T.D)

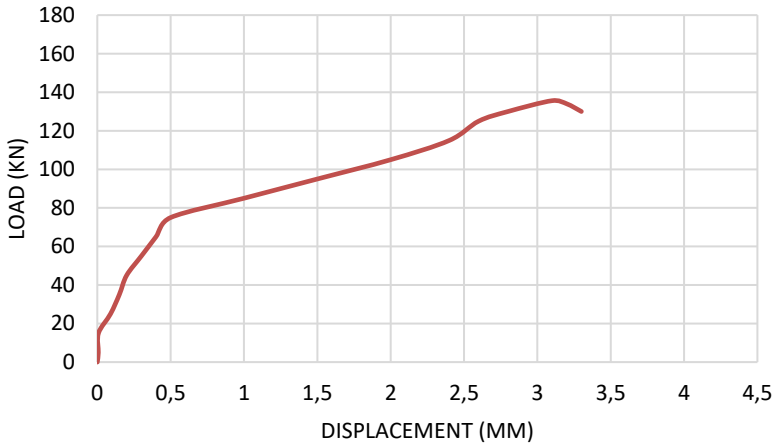

Fig. 16. specimen (S. T.D) Load-Displacement

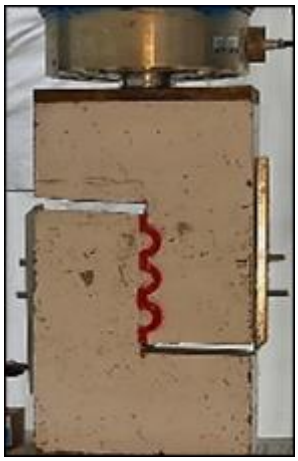

Fig. 17. specimen (S. C.D)

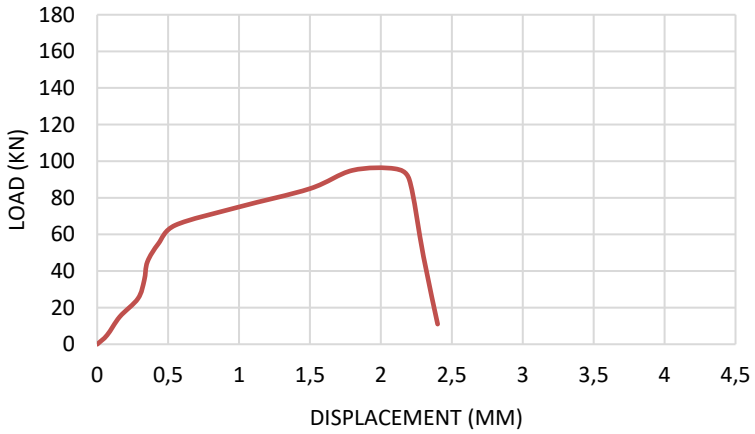

Fig. 18. specimen (S. C.D) Load-Displacement

4.3. Failure Modes

During the experimental observations, it was noted that the failure behavior of the tested specimens varied considerably. Some specimens exhibited sudden shear failure, whereas others showed a more gradual and controlled failure process accompanied by larger deformation. The failure characteristics can be categorized according to the strengthening groups as follows:

Specimens strengthened with interface grooves showed noticeable improvements in shear behavior compared with the reference specimens. Among these configurations, the rectangular groove specimen (S.R) exhibited the highest shear capacity and energy absorption, followed by the triangular groove specimen (S.T), while the circular groove specimen (S.C) showed comparatively lower strength. These results indicate that the geometry of the grooves significantly affects the mechanical interlocking mechanism and consequently the shear transfer across the interface.

The hybrid strengthening technique combining bolts with interface grooves produced the best overall structural performance among all tested groups. In particular, the specimens with rectangular grooves combined with bolts exhibited the highest load capacity and energy absorption. Specimen S.R.D2 achieved the best performance, recording the highest ultimate load and energy absorption among all specimens. These results demonstrate that combining mechanical interlocking (grooves) with mechanical connectors (bolts) provides a highly effective mechanism for improving both shear strength and energy dissipation capacity as illustrated in Figure (19).

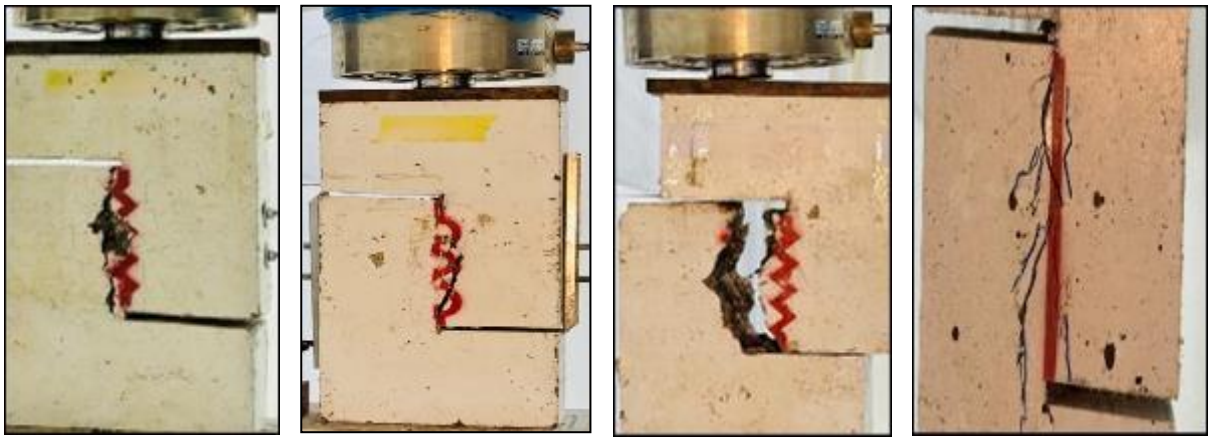

Fig. 19. Failure modes

5. Conclusions

The experimental study revealed that interface groove geometry is a very important factor in the regulation of the shear nature and structural performance of the experimented specimens. These findings are clear evidence that the shear transfer mechanism can be greatly improved by changing the interface configuration to increase the mechanical interlocking and slow down crack propagation. The rectangular groove shape is among the specimens that were tested had the highest structural performance with regards to shear capacity, stiffness and energy absorption. The initial crack in this specimen occurred at an approximate load of 60 kN and the final load was about 131 kN, the maximum load carrying capacity of any of the configurations tested. Besides, the specimen recorded an ultimate displacement of around 2.2 mm, energy absorption capacity of around 261 J, and ductility index of 11.0. These findings affirm that the rectangular interface geometry was highly mechanically interlocked, and that such a reinforcement made the interfaces substantially more effective in transferring shear across the interface and helping to maintain a more consistent failure behavior. The triangular groove design (S.T) also exhibited significant increase in shear resistance with respect to the rest of the specimens. The initial crack to be seen on this specimen was at around 45 kN, and the maximum load was about 105.86 kN. The ultimate displacement of the specimen was about 1.8 mm, energy absorption capacity was about 145 J, and ductility index was 9.0. These findings prove that the triangular groove pattern provided a satisfactory balance between shear strength and deformation capacity. The triangular geometry assisted in good distribution of stress on the interface that enhanced the shear resistance and also ensured that the deformation behavior was relatively stable before failure. Conversely, the circular groove pattern (S).C) exhibited another structural response as compared to the other configurations. The initial crack occurred at about 35 kN, and the final load was about 65.97 kN that is the lowest shear capacity of the tested specimens. Nevertheless, the circular groove specimen had the greatest deformation capacity with ultimate displacement of about 2.4 mm and ductility index of 12.0, and energy absorption capacity of approximately 118 J. The findings point to the fact that the circular groove design offered a decreased shear strength, but it enhanced the ductility of the specimen and enabled it to be deformed to a higher degree before breaking down. The mechanical interlocking was enhanced to a certain degree by the curved geometry of the grooves and also produced gradual crack formation and more controlled failure behavior. All the conclusions in the experiment indicate that the geometry of the interface is conclusive in enhancing shear transfer efficiency and structural performance. The rectangular groove structure was found to be the most effective in performance in shear strength and energy absorption whereas the triangular structure offered a balanced structural behavior of strength and deformation. At the same time, the circular groove design exhibited better ductility but less shear capacity. The findings indicate the significance of maximizing the interface geometries in reinforced concrete structures that are enhanced with modern materials like SIFCON. This optimization can be used to increase shear resistance, augment energy dissipation capability and help achieve safer and more reliable structural performance in practice.

Acknowledgments

The author sincerely extends gratitude to the staff of the Civil Engineering Department at the University of Karbala for their dedicated efforts and steadfast support throughout this research. Their assistance and provision of all necessary facilities were instrumental in enabling the successful completion of this study.

References

[1] Lankard DR. Slurry-Infiltrated Fiber Concrete (SIFCON): Properties and Applications. MRS Proceedings; 1984. https://doi.org/10.1557/PROC-42-277
[2] Wang ML. Shear properties of slurry-infiltrated fibre concrete (SIFCON). Construction and Building Materials. 1994;8(5):281-287. https://doi.org/10.1016/S0950-0618(09)90029-0
[3] Al-Rousan RZ, et al. Shear repairing and strengthening of reinforced concrete beams using SIFCON. Case Studies in Construction Materials. 2018. https://doi.org/10.1016/j.istruc.2018.05.001
[4] Sampath P, et al. Mechanical properties of slurry-infiltrated fibrous concrete (SIFCON). Materials Today: Proceedings. 2020. https://doi.org/10.1016/j.matpr.2019.12.401
[5] Akçaözoğlu K. The effect of curing conditions on the mechanical properties of SIFCON. Revista de la Construcción (English Edition). 2021.
[6] Robayo-Salazar R, et al. Slurry-Infiltrated Fiber Concrete (SIFCON) for use in ballistic and blast-resistant applications. Case Studies in Construction Materials. 2023. https://doi.org/10.1016/j.istruc.2023.105282
[7] Ali MH, et al. Mechanical properties and efficiency of SIFCON samples under elevated temperature. Journal of Building Engineering. 2022. https://doi.org/10.1016/j.cscm.2022.e01281
[8] Ghani LA, et al. Preparation and engineering properties of Slurry Infiltrated Fiber Concrete (SIFCON). Regional Journal of Engineering Studies. 2024.
[9] Al-Hadithi AI. Investigating mechanical properties of SIFCONs produced with different fiber aspect ratios. Cement & Concrete Composites. 2024. https://doi.org/10.1016/j.conbuildmat.2024.138220
[10] ETASR. Bond performance of the slurry infiltrated fiber concrete overlay to normal strength concrete substrate. Engineering, Technology & Applied Science Research (ETASR).
[11] Ipek S, Tuyan M, Yazici H. Effects of fiber content and geometry on SIFCON performance. Construction and Building Materials. 2014.
[12] Naaman AE, et al. Early studies on high-fiber cement composites and their bonding behavior. Cement and Concrete Research. 1987.
[13] Stiel L. Investigation of SIFCON microstructure and fiber-matrix interaction. Journal of Materials in Civil Engineering. 2004.
[14] Tuyan M, Yazıcı H. SIFCON behavior under dynamic/impact loading-experimental study. International Journal of Impact Engineering. 2012.
[15] Iqbal M, et al. Vacuum mixing influence on slurry infiltration and porosity of SIFCON. Cement & Concrete Research. 2019.
[16] Graybeal B. Material property characterization of ultra-high-performance concrete (UHPC). FHWA; 2006.
[17] Balázs WKTGL. Impact and blast resistance of slurry infiltrated fiber concrete - review. Periodica Polytechnica Civil Engineering / FIB review. 2023.
[18] Tuama WK. Punching shear strengthening of flat slabs using SIFCON. ResearchSquare; 2025. https://doi.org/10.21203/rs.3.rs-7002488/v1
[19] Robles J, et al. SIFCON jacketing technique for strengthening shear-deficient beams: experimental and numerical study. Engineering Structures. 2015.
[20] Rossi P. Influence of fibre geometry and matrix maturity on mechanical performance of UHPC and SIFCON-like composites. Cement and Concrete Composites. 2013. https://doi.org/10.1016/j.cemconcomp.2012.08.005
[21] Graybeal B. Material characterization of fiber-reinforced cement composites. FHWA-HRT-06-103; 2006.
[22] Ipek S, et al. Pullout behavior of steel fibers in high-slurry matrices and implications for bond in SIFCON. Construction and Building Materials. 2016.
[23] Wang M, Naaman AE. Shear and torsion behavior of fiber-reinforced cementitious composites. Journal of Structural Engineering. 1997.
[24] Al-Rousan RZ, Al-Hayek R. Use of SIFCON jackets for retrofitting corroded/deficient RC members. Journal of Performance of Constructed Facilities. 2019.
[25] Ipek S, Yazici H. Effect of fiber volume fraction and aspect ratio on SIFCON fracture energy. Materials and Structures. 2018.
[26] Ghoniem Y, et al. Multiscale modelling of SIFCON: from microstructure to macroscopic behavior. Cement & Concrete Composites. 2020.
[27] Ain Shams Engineering Journal / ETASR. An experimental study on SIFCON overlays and interface preparation: Bond strength, surface roughness, bonding agents. 2021.

[28] Ipek S, Tuyan M, Yazıcı H. SIFCON under cyclic loading-fatigue resistance and crack bridging. International Journal of Fatigue. 2012.
[29] Naaman AE, Reinhardt H. Fiber-bridging mechanisms and toughening in high-fiber composites. Journal of Materials in Civil Engineering. 1987.
[30] MDPI. Development of an Engineered Slurry-Infiltrated Fibrous Concrete: Experimental and Modelling Approaches. Materials. 2024.
[31] Algın Ö, Özbebek A, Gerginci A, Mermerdaş K. Effects of Basalt Fibre Utilization on Durability and Mechanical Properties of SIFCON. Construction and Building Materials. 2020;237.